



Sustainable route to hydrogen – Design of stable catalysts for the steam gasification of biomass related oxygenates

B. Matas Güell, I.M. Torres da Silva, K. Seshan^{*}, L. Lefferts

Catalytic Processes & Materials, Faculty of Science and Technology, University of Twente, PO Box 217, 7500 AE Enschede, The Netherlands

ARTICLE INFO

Article history:

Received 9 July 2008

Received in revised form 16 September 2008

Accepted 19 September 2008

Available online 27 September 2008

Keywords:

Steam reforming

Acetic acid

Hydrogen

Nickel based catalyst

Sustainable

ABSTRACT

Steam reforming of acetic acid, a biomass derived oxygenate, has been studied over Ni-based catalysts. Ni/ZrO₂ showed gradual deactivation in time. Coke formation as well as a competitive adsorption of reactants is suggested to be responsible for the catalyst deactivation. Addition of potassium strongly influenced the reduction temperature of NiO. The presence of potassium and lanthanum improved catalyst stability by decreasing coke accumulation. It is proposed that the presence of lanthanum as an oxy-carbonate phase enhances coke gasification.

© 2008 Elsevier B.V. All rights reserved.

1. Introduction

Environmental friendly energy is a major goal in our society [1]. Over the past few years, hydrogen has aroused tremendous interest as an energy carrier. Currently, one of the limitations of hydrogen generation is that it is based on fossil fuels, leading to a net production of greenhouse gases [2]. Thus, the use of biomass as an alternative hydrogen source, with CO₂-neutral impact, may become important in the future.

Solid biomass can be converted into a liquid bio-oil, via the so called flash pyrolysis process, a convenient feedstock for further processing. This also makes storage and transport of biomass based feedstocks more effective. Gasification of bio-oil is a promising route for syngas (CO + H₂) generation from biomass. However, it is energy intensive and requires temperatures around 1250 °C [3]. Milder conditions can be applied in the presence of a catalyst (750–900 °C) [4]. Dolomite, alkali metal and nickel-based catalysts are the most common catalysts reported for gasification of biomass [5]. However, severe coking and deactivation is a major problem for both biomass and bio-oil gasification [3–6]. Design of a stable catalyst is still an open challenge.

In previous studies on the steam reforming of biomass related oxygenates, particularly acetic acid (AcOH), we have reported that

supported Pt catalysts show excellent activity [6,7]. However, condensation of intermediate oxygenates formed (e.g., acetone), during reaction, on the support led to oligomers and coke formation. These species blocked the catalytic active sites, resulting in deactivation. [7]. Such polymerization cannot be avoided [6] and the strategy to overcome catalyst deactivation is to minimize such oligomers and coke accumulation. Regeneration of the catalyst periodically, is one option. In this case, the oligomers/coke accumulated on the catalyst are combusted in air. This results in discontinuous operation as the reaction is stopped during the regeneration step and catalyst lifetime, reported currently [7], is too short to do this on a commercial scale. Another possible approach is to remove coke as it is formed, by *in situ* regeneration (combustion) during reaction, similar to autothermal reforming, or by enhancing the steam reforming activity, thus minimizing coke/oligomer accumulation. In our case, the approach was chosen to limit coke accumulation, during steam reforming of acetic acid, by enhancing the steam reforming activity, and attempt to steam reform the relatively unreactive deposits such as oligomers.

In an earlier study [8] a bifunctional mechanism has been proposed for Pt/ZrO₂ catalyst, where both Pt and support participate in the acetic acid (AcOH) to syngas conversion. AcOH is suggested to be activated on Pt and water is activated on ZrO₂. Water activation is the demanding step; enhancement of water sorption/activation is essential in order to increase the steam reforming activity. It is known [9,10] that Ni, in contrast to Pt, is able to activate H₂O via formation of NiO. Ni/ZrO₂ was selected for

^{*} Corresponding author.

E-mail address: k.seshan@utwente.nl (K. Seshan).

this study with the basis that both Ni and zirconia can contribute to water activation during steam reforming.

In general, stability of Ni-based catalysts is hindered by coke formation, sometimes including carbon-nano-fibers, as well as sintering of the metal particles during reaction [11]. Markevich et al. [12] studied the steam reforming of sunflower oil over Ni/Al catalysts between 550 and 650 °C. Nickel particle size increased by a factor of 4 after 12 h time on stream (TOS), causing catalyst deactivation. On the other hand, Kechagiopoulos et al. reported deactivation due to coke deposition during steam reforming of biomass based oxygenates over Ni-based catalysts at similar temperatures (600–750 °C) [13]. An exhaustive review on the gasification of biomass and related feedstocks, including Ni-based catalysts, has been presented by Ross and co-workers [5].

There is tremendous amount of information available on the design of effective Ni-based catalysts for steam reforming of methane [14,15]. Modification with alkali/alkaline earth metals (e.g., K, Na, Ca) and rare earths (La) is reported to result in enhanced activity and stability [5,14,15]. Alkali metals are suggested to enhance gasification activity by assisting in the formation of OH groups on oxide supports [10,14,16]. In our case, therefore, addition of potassium to Ni/ZrO₂ may improve catalyst stability by gasifying carbonaceous species deposited on the catalyst surface. It is further suggested that, in the case of dry reforming of CH₄, lanthanum forms oxygen-containing species (La₂O₂CO₃) during reaction which help combust coke accumulated on the catalyst [17,18]. La is also known to stabilize metal particles and oxides by preventing sintering [19,20].

Despite this extensive research on the modification of Ni-based catalysts for steam reforming of alkanes, very little work has been reported concerning steam reforming of biomass based oxygenates, e.g., acetic acid [21,22]. Basagiannis and Veykios [21] studied the influence of reaction temperature and catalytic material on acetic acid steam reforming over Ni supported on La₂O₃ and/or Al₂O₃. The role of lanthana is, according to them, to form oxycarbonate type species (La₂O₂CO₃) which helps minimize coke accumulation, as mentioned earlier. However, no results on the stability of the catalysts are shown. Román Galdámez et al. also studied the influence of La on the catalytic and mechanical properties of Ni/Al₂O₃ catalysts. They did not observe any improvement by the presence of La on hydrogen yields.

Aim of this investigation is to explore the effect of lanthanum and potassium promoters on activity and stability of Ni/ZrO₂ for steam reforming of acetic acid. Development of a stable catalyst for the steam reforming of acetic acid as a model compound is a first step towards stable catalysts for steam reforming of flash pyrolysis based bio-oil.

2. Experimental

2.1. Catalyst preparation

ZrO₂ (monoclinic, Daiichi Kigenso Kagaku Kogio, RC 100) was first calcined for 15 h at 850 °C (heating rate 5 K min⁻¹) in flowing air (30 ml min⁻¹). It was then crushed and sieved to give grains of 0.3–0.6 mm. The grains were impregnated with 0.1 M Ni(NO₃)₂·6H₂O (Alfa Aesar) solution to load ZrO₂ with 3.5 wt.% Ni. The catalyst was dried at 70 °C for 4 h in a rotary evaporator followed by drying overnight at 120 °C and, eventually, calcined at 725 °C for 15 h (heating rate 5 K min⁻¹) in flowing air (30 ml min⁻¹). Hereafter, this catalyst is denoted as Ni/ZrO₂.

K and La-doped catalysts, 3.5 wt.%Ni/2% K-ZrO₂, 3.5 wt.%Ni/5 wt.%La-ZrO₂ and 3.5 wt.%Ni/2 wt.% K-5 wt.%La-ZrO₂, were also prepared via wet impregnation. K and La were added to ZrO₂ by using KNO₃ and La(NO₃)₃·6H₂O solutions, respectively. After impregna-

tion, the supports were dried using a rotary evaporator followed by drying overnight at 120 °C. Once dried, the doped supports were first calcined at 600 °C for 4 h and then loaded with 3.5 wt.% Ni. All three catalysts were finally calcined for 15 h at 725 °C.

Hereafter, these catalysts are denoted as Ni/K-ZrO₂, Ni/La-ZrO₂ and Ni/K-La-ZrO₂.

2.2. Catalyst characterization

The elemental composition of the catalysts was determined with X-ray fluorescence spectroscopy (XRF) (Phillips PW 1480 spectrometer). Specific surface area measurements were carried out with N₂ adsorption–desorption at 77 K in a Micromeritics TriStar instrument, applying the BET adsorption isotherm.

Nickel particle size was determined with two different techniques: X-rays diffraction (XRD) and scanning transmission electron microscopy–energy dispersive X-ray analysis/electron energy loss spectroscopy (STEM–EDX/EELS). XRD patterns were recorded with a Philips X'Pert APD using Cu Kα radiation. Spectra were registered with 2θ between 5° and 80°. The mean Ni particle diameter was estimated by X-ray line broadening analysis (XLBA) using the Scherrer equation.

Catalyst reducibility was probed with a home made temperature-programmed reduction (TPR) equipped with a standard thermoconductivity detector. For this purpose, 300 mg of catalyst sample was pretreated in Ar at 700 °C for 5 min. After pretreatment, the sample was first cooled down to room temperature in Ar and then heated to 800 °C at a rate of 5 °C min⁻¹ in a 5%H₂/Ar flow (30 ml min⁻¹).

Thermogravimetry (TG, Mettler Toledo) was used to quantify the amount of carbon deposited on the catalysts after reaction. The samples were heated from room temperature to 800 °C at 5 °C min⁻¹ in air.

2.3. Catalytic testing

For catalytic experiments, 50 mg of catalyst diluted with quartz particles with grains of 0.3–0.6 mm (ratio 1:1) was loaded in an alumina fix-bed reactor (4 mm i.d.) and held in place by quartz wool plugs. The catalyst was first reduced *in situ* in 5%H₂/N₂ flow (50 ml min⁻¹) at 650 °C for 1 h. After purging with N₂ for 15 min, the temperature was increased to 700 °C. An aqueous solution of acetic acid with a steam to carbon molar ratio (S/C) of 5 was delivered by means of a pulse-free syringe pump (Isco Model 500 D). This solution was evaporated at 190 °C and provided to the system via a pre-heater (cylinder, i.d. 50 mm, length 150 mm, packed with quartz wool). The mixture was diluted with nitrogen, which was used both as an inert carrier gas and as internal standard. The gas feed, consisting of 2.5%CH₃COOH (3 ml min⁻¹)/25%H₂O (30 ml min⁻¹)/balance N₂, was introduced to the fix-bed reactor. The total gas hourly space velocity (GHSV) was calculated on a volume basis.

The composition of the reactant/product mixture was determined with an on-line gas chromatograph (GC, Varian CP-3800) equipped with (i) two thermal conductivity detectors (TCD), for the quantification of permanent gases, and a flame ionization detector (FID) for quantification of the hydrocarbons and (ii) the following columns for separation: Hayesep Q, Hayesep T, Molsieve 13X, Molsieve 5A and CP-Wax 52CB.

Acetic acid conversion was calculated as the moles of acetic acid reacted divided by the moles of acetic acid fed.

The hydrogen yield was defined as the percentage of the maximum amount of hydrogen that can be produced, based on the following reaction:

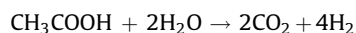


Table 1

Catalysts elemental analysis and BET surface area of fresh samples.

Catalyst	Content (wt.%)			Surface area (m ² /g)
	Ni	La	K	
Ni/ZrO ₂	3.65	–	–	35
Ni/La-ZrO ₂	3.44	4.27	–	33
Ni/K-ZrO ₂	3.16	–	1.07	27
Ni/K-La-ZrO ₂	3.36	4.29	0.90	25

Table 2

Mean NiO particle size calculated by XRD for catalysts before and after reaction.

Catalyst	Crystallite diameter (nm)	
	Before reaction	After reaction
Ni/ZrO ₂	20	21
Ni/La-ZrO ₂	22	16
Ni/K-ZrO ₂	20	10
Ni/K-La-ZrO ₂	16	15

For carbon-containing compounds, the yields were calculated based on C₁ equivalent values; e.g., CO and CO₂ yields were calculated as one time the number of moles produced divided by two times the number moles of acetic acid fed.

3. Results

3.1. Catalyst characterization

Elemental analysis and the specific surface area of the Ni-based catalysts are shown in Table 1. In general, Ni loadings were in the range intended for preparation (3.5%). In the case of K, only about 50% of the intended amount was retained in the catalyst. Lanthanum amounts were as expected. Lanthanum addition did not significantly influence the total surface area of the catalysts, whereas K addition caused a slight decrease. Table 2 compares mean NiO particle sizes as obtained from XRD–XLBA measurements.¹ Only minor differences in the mean particle size were observed. STEM–EDX/EELS measurements (not shown) confirmed the order of magnitude of the size of the NiO particles.

Experimental results of hydrogen consumption during TPR of the Ni-based catalysts are shown in Fig. 1. TPR profile of Ni/ZrO₂ (Fig. 1a) exhibited three reduction peaks with maxima at 190, 250 and 350 °C, respectively. Addition of lanthanum (Fig. 1b) shifted all the peaks to higher temperatures. Potassium doping (Fig. 1c) resulted in a completely different reduction profile. A small broad peak centered around 370 °C and a larger, second peak at 595 °C were observed. The spectrum corresponding to the catalyst containing both potassium and lanthanum (Fig. 1d), displayed practically the same profile as the catalyst doped with K only. In both cases (Fig. 1c and d) the main peak is shifted to much higher temperatures, as compared to catalysts without K (Fig. 1a and b). It is important to note that the total peak area corresponds well with the amount of H₂ required for the reduction of NiO to Ni in all catalysts.

3.2. Catalyst testing

The catalytic performance of the Ni/ZrO₂ based catalysts in the steam reforming of acetic acid is compared in Figs. 2 and 3 in terms of H₂ yield and acetic acid conversion, respectively. A commercial Ni-based pre-reforming catalyst was used as a reference. Regard-

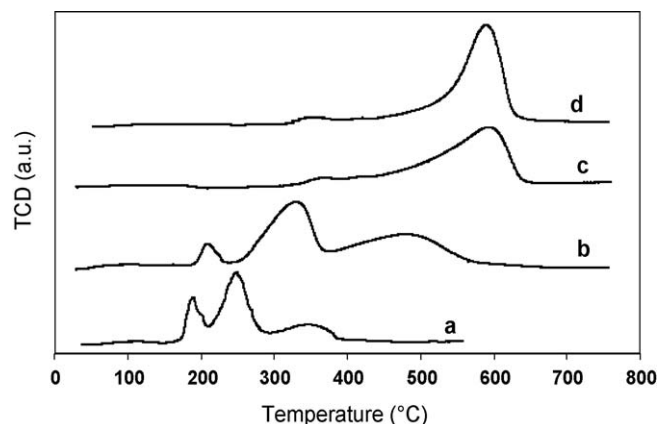


Fig. 1. TPR profiles for (a) 3.5%Ni/ZrO₂; (b) 3.5%Ni/La-ZrO₂; (c) 3.5%Ni/K-ZrO₂ and (d) 3.5%Ni/K-La-ZrO₂.

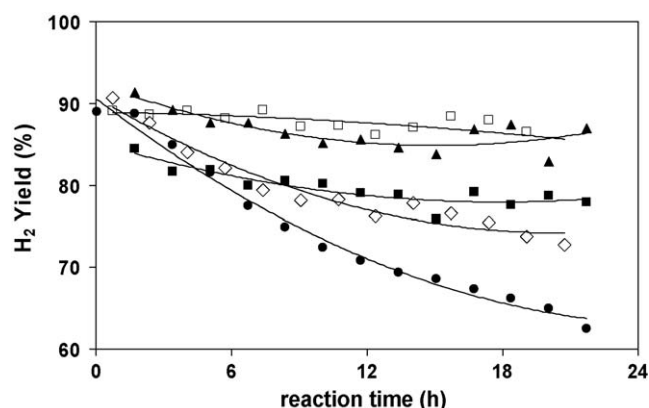


Fig. 2. H₂ yield vs. time on stream for the steam reforming of AcOH over (●) 3.5%Ni/ZrO₂; (□) 3.5%Ni/La-ZrO₂; (◇) 3.5%Ni/K-ZrO₂; (▲) 3.5%Ni/K-La-ZrO₂; (■) Commercial. (Reaction conditions: 700 °C, S/C = 5, GHSV = 240,000 h⁻¹).

ing the hydrogen production, all Ni catalysts showed very high initial activity, with H₂ yields close to thermodynamic equilibrium composition (87%). The Ni/ZrO₂ catalyst deactivated the most, with H₂ yields dropping from 87% to 62% during 22 h. Ni/K-ZrO₂ showed slightly improved performance, but still deactivated with time. The two lanthanum-promoted catalysts showed the best results. These catalysts were reasonably stable and lost only about 7% H₂ yield in 20 h time on stream. These catalysts were more active than the

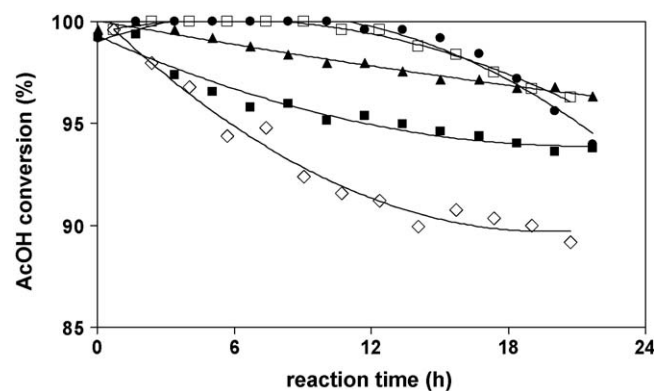


Fig. 3. AcOH conversion vs. time on stream for the steam reforming of AcOH over (●) 3.5%Ni/ZrO₂; (□) 3.5%Ni/La-ZrO₂; (◇) 3.5%Ni/K-ZrO₂; (▲) 3.5%Ni/K-La-ZrO₂; (■) Commercial. (reaction conditions: 700 °C, S/C = 5, GHSV = 240000 h⁻¹).

¹ It is important to note that the relative comparison of nickel particle size before and after reaction was based on the size of NiO particles after oxidation of the fresh and used catalysts (oxidation during regeneration).

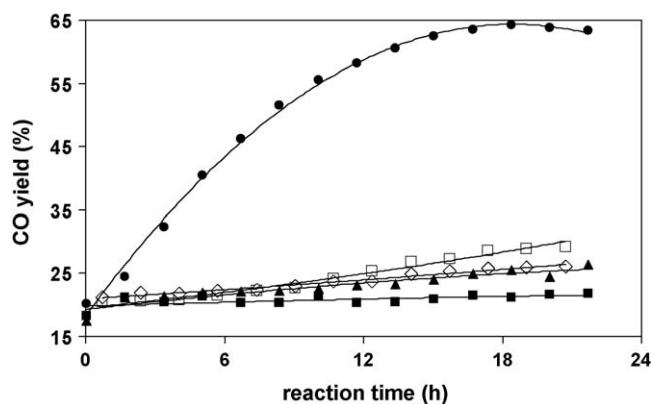


Fig. 4. CO yield vs. time on stream for the steam reforming of AcOH over (●) 3.5%Ni/ZrO₂; (□) 3.5%Ni/La-ZrO₂; (◇) 3.5%Ni/K-ZrO₂; (▲) 3.5%Ni/K-La-ZrO₂; (■) Commercial. (Reaction conditions: 700 °C, S/C = 5, GHSV = 240,000 h⁻¹).

commercial catalyst, even after 20 h time on stream, and stabilities were comparable.

Acetic acid conversions were, in all cases (Fig. 3), complete (close to 100%) during the first minutes of the reaction and decreased slowly with time on stream. Carbon balance was reasonable in all the experiments and was $100 \pm 5\%$. Further, all catalysts showed a gradual increase in CO formation with time (Fig. 4), with a simultaneous decrease in CO₂ yield (Fig. 5) and H₂ yield (Fig. 2). This effect was especially pronounced in the case of the unpromoted catalyst. CH₄ formation was negligible in all cases.

3.3. Catalyst characterization after use

In order to establish the cause of catalyst deactivation, coke deposition as well as metal sintering was investigated. The amount of coke accumulated on the catalysts during 22 h TOS at 700 °C was determined with thermo-gravimetric analysis (Table 3). Typically coke burn off occurred around 500 °C for all the catalysts. The smallest amount of coke deposition was found over Ni/K-La-ZrO₂ (0.7 wt.%). The carbon accumulated in the case of the Ni/La-ZrO₂ was 1.5% and in the case of Ni/K-ZrO₂ catalyst was higher (2.8 wt.%). Finally, Ni/ZrO₂ catalyst accumulated the highest amount of deposits (6.5 wt.%). These results show that the presence of K and La reduces the amount of accumulated deposits remarkably. TEM and SEM studies of spent catalyst revealed the presence of both filamentous carbon as well as carbon encapsulating Ni particles (not shown).

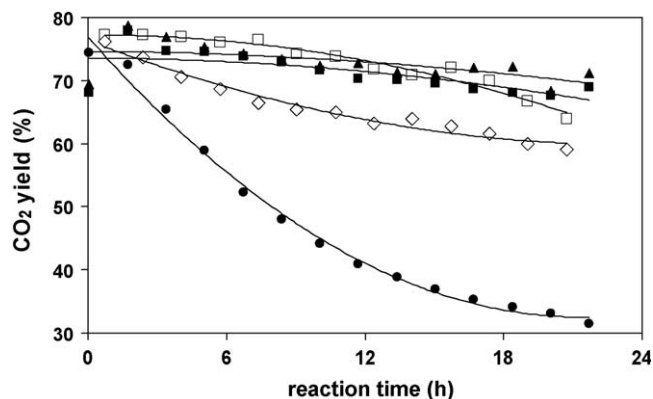


Fig. 5. CO₂ yield vs. time on stream for the steam reforming of AcOH over (●) 3.5%Ni/ZrO₂; (□) 3.5%Ni/La-ZrO₂; (◇) 3.5%Ni/K-ZrO₂; (▲) 3.5%Ni/K-La-ZrO₂; (■) Commercial. (Reaction conditions: 700 °C, S/C = 5, GHSV = 240,000 h⁻¹).

Table 3

Coke amount after 22 h time on stream over: (●) 3.5%Ni/ZrO₂, (□) 3.5%Ni/La-ZrO₂, (◇), 3.5%Ni/K-ZrO₂, (▲) 3.5%Ni/K-La-ZrO₂.

Catalyst	Coke amount (%)
Ni/ZrO ₂	6.5
Ni/La-ZrO ₂	1.5
Ni/K-ZrO ₂	2.8
Ni/K-La-ZrO ₂	0.7

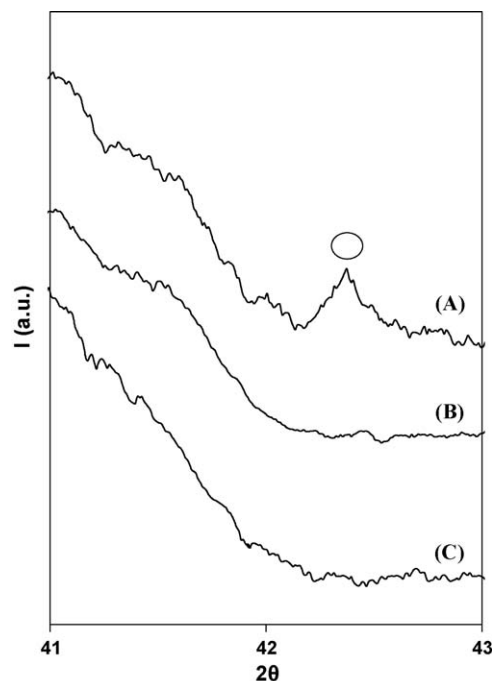


Fig. 6. XRD patterns of (A) used Ni/La-ZrO₂; (B) fresh Ni/La-ZrO₂; (C) Used Ni/ZrO₂ given for comparison; Symbol (o) corresponds to La₂O₂CO₃.

Comparison of NiO particles size for both fresh and spent catalyst is shown in Table 2. Particle size did not increase during use in the case of Ni/ZrO₂ catalysts. A slight decrease was observed in the case of the modified Ni-based catalysts. Therefore, none of the catalysts suffered from metal sintering.

XRD measurements on fresh and used Ni/La-ZrO₂ confirmed the presence of La₂O₂CO₃ based on the existence of a diffraction peak at $2\theta = 42.3^\circ$ (Fig. 6) exclusively on the spent Ni/La-ZrO₂ catalyst. Similar trend was observed for the spent Ni/K-La-ZrO₂ (not shown). Typically, XRD measurements on spent catalyst after regeneration (Fig. 7(A)) show the presence of NiO at $2\theta = 43.4^\circ$, similar to fresh catalyst (Fig. 7(A)), in contrast to spent catalyst without regeneration (Fig. 7(B)).

4. Discussion

One of the major problems with steam reforming reactions is coke deposition which blocks active sites and leads to catalyst deactivation [9,23]. Metal sintering, on the other hand, may also cause catalyst deactivation, decreasing the number of active sites [12]. In this study, we have used acetic acid as a “model biomass oxygenate” to determine catalyst stability during steam gasification. Our results (Figs. 2 and 3) show very active catalysts, with complete AcOH conversion at initial times on stream. Similar trends have been stated in literature. Román Galdámez et al. also reported high AcOH conversions (85%) using higher Ni loadings (8%Ni-Al-La) at 650 °C but under comparable S/C ratio (5.58) and

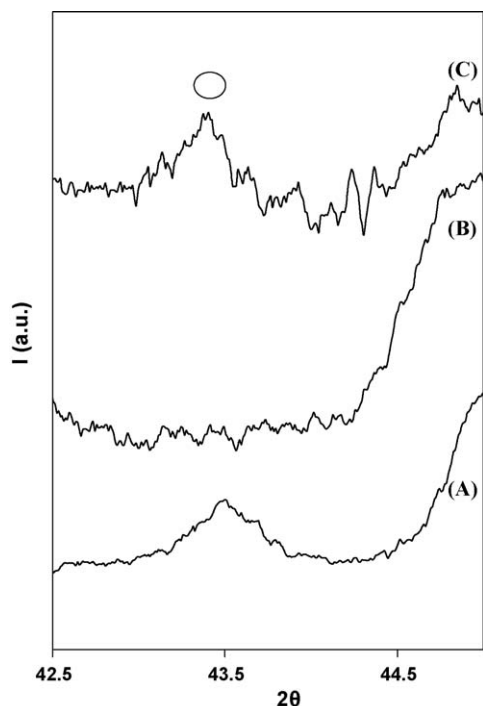


Fig. 7. XRD patterns of 3.5%Ni/La-ZrO₂ (A) before reaction; (B) after reaction and (C) after regeneration. (o) NiO.

space velocity conditions. However product distribution in their case did differ from our findings. They observed lower amounts of H₂ and CO₂ and higher amounts of CO and CH₄. On the other hand, Basagiannis and Veykios [21] showed that when a 17% Ni/La₂O₃/Al₂O₃ catalyst was used under the same reaction temperature (700 °C) and similar S/C (6) and space velocities, AcOH was only converted 60%. This clearly indicates higher catalyst activities in our case, however, with different profiles of (continuous) deactivation of the non/modified Ni/ZrO₂ catalyst. In addition, the deactivation is also accompanied by changes in the CO/CO₂ ratio, which increases during time on stream. The increase in the CO/CO₂ ratio is accompanied by a decrease in H₂ production. This suggests an influence on the ability of the catalysts for the WGS reaction.

Observations on metal particle size did not show any metal sintering with or without promoters. Therefore, metal sintering is excluded as a cause of catalyst deactivation in our case. Under similar temperature conditions (550–650 °C), Markevich et al. [12] observed an increase of nickel particles during steam reforming of sunflower oil over Ni supported on hydrotalcites type materials. The discrepancy between both investigations could be attributed to catalyst type and reaction.

According to our results (Fig. 2 and Table 3), there is, as suggested above, a direct correlation between coke accumulated on the catalyst and its performance. The more the coke deposited on the catalyst, the more severe the deactivation of the catalyst is; i.e., lower hydrogen yields with time on stream. In previous studies [6] we showed that on ZrO₂, AcOH was converted first into acetone which subsequently led to oligomer/coke formation *via* condensation/dehydration reactions involving mostly diacetone alcohol, mesityl oxide and ketene [7]. The complete conversion of AcOH during the first 10 h of reaction suggests that part of the catalyst bed is enough to steam reform AcOH. This fact along with coke formation suggests an increase in “C” buildup over the catalyst bed with time on stream. This would decrease the number of active sites for both steam reforming as well as WGS reactions. With

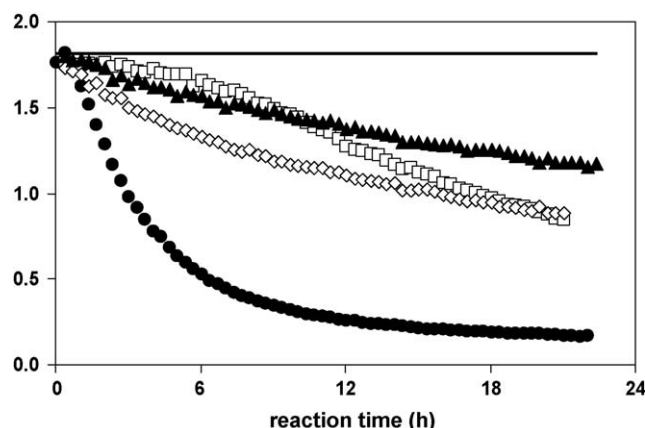


Fig. 8. [CO₂][H₂]/[CO] ratio vs. time on stream for the steam reforming of AcOH over (●) 3.5%Ni/ZrO₂; (□) 3.5%Ni/La-ZrO₂; (◇) 3.5%Ni/K-ZrO₂; (▲) 3.5%Ni/K-La-ZrO₂. (Reaction conditions: 700 °C, S/C = 5, GHSV = 240,000 h⁻¹).

regards to WGS reaction, calculations of the ratio [CO₂][H₂]/[CO] are shown in Fig. 8. It can be seen that the WGS reaction is at equilibrium only in the initial stage. The product mixture moves further away from the equilibrium with time on stream, indicating deactivation of the catalyst for WGS during time-on-stream. This phenomenon is especially pronounced in the case of Ni/ZrO₂. It is known in literature [24–27] that Ni-based catalysts show very poor activity (TOF) for WGS reaction but are very active for steam reforming. Further, the deactivation curves in Figs. 2 and 3 indicate that only part of the Ni/ZrO₂ catalyst bed is sufficient to keep the near complete steam reforming conversion, as discussed above. The result in Fig. 8 reveals that the catalyst deactivates much faster for WGS.

Promotion of the Ni/ZrO₂ catalyst shows promise, as evidenced in this study. All modified catalysts exhibit less severe deactivation. The combination of both promoters results in the most stable catalyst for WGS (Fig. 8).

It has been reported [28] that addition of potassium to Al₂O₃ supported catalysts enhanced coke gasification during biomass steam reforming. No catalyst deactivation was observed for K modified catalyst used for wood gasification, even after 30 h time on stream. Little or no carbon was found on the used catalyst. Those results are in line with our observation. It has been proposed in literature [10] that the presence of alkali induces a strong electric field in its vicinity, enhancing water dissociation and facilitating formation of reactive hydroxyl groups. The increase in water activation for potassium doped catalysts as compared to the case in which the alkali is not present might result in enhanced steam reforming/preventing of the carbon deposits, thus reducing coke deposition. Indeed higher ethanol steam reforming activity was observed when potassium was added in Ni/MgO [29]. However, the enhanced steam reforming activity could not be observed in our experiments as the products yields were close to thermodynamic equilibrium at initial time on stream.

In addition, it is important to point out the strong influence of potassium on the reduction temperature of NiO, making it more difficult. In literature, there is a debate about the role of alkalis in the reduction of NiO. Some authors [29,30] have shown that potassium promotes the reduction of NiO, supported on MgO. Contrary to this and in line with our observations, it has been reported that addition of potassium retards the reduction process by impeding the dissociation of H₂ or by blocking of the pores by potassium compounds, limiting H₂ accessibility or preventing H₂O to leave the reduced metal site [31,32].

Catalyst stability was further improved by adding lanthanum. The amount of carbon deposits determined by TGA (1.5%) clearly indicates that presence of lanthanum lowers carbon accumulation. Basagiannis and Veykios [21] observed similar trends, quantifying only 0.43% carbon over Ni/La₂O₃/Al₂O₃ after steam reforming of AcOH for 2 h at 700 °C. The positive influence of lanthanum has been reported in literature [17,18,26]. Olsbye et al. [33] reported that, under dry reforming of CH₄ conditions, the addition of 1.7 wt.% La to 0.15 wt.% Ni/Al₂O₃ decreased coke formation by almost 50%. They could partially explain these results based on the different Ni cluster size of the promoted and un-promoted catalysts: the larger the Ni cluster the more the carbon deposition. They also speculated that the presence of La leads to the formation of mixed phases with cationic vacancies which enhance mobility of lattice oxygen anions. In this way, surface reaction between carbon-containing species and reactive oxygen species is favored.

According to Zhang and Veykios [17] and Guo et al. [18], formation of coke during dry reforming of CH₄ over Ni/La₂O₃ catalysts, is hindered by the presence of lanthanum as La₂O₂CO₃. This oxy-carbonate phase, which should be the result of the reaction between La₂O₃ and CO₂ (product of gasification), is suggested to limit the formation of encapsulating carbon layer around the Ni particles and, thus, minimizing deactivation [16,17]. It is further suggested that due to the synergetic sites which consist of Ni and La, the carbon species formed on the Ni sites would be favorably removed by the oxygen species originating from La₂O₂CO₃. Indeed, a close look at the XRD patterns (see Fig. 6) shows the presence of the oxy-carbonate phase of lanthana in the catalyst after use. As expected, this phase was absent in a Ni/ZrO₂ and a fresh Ni-La/ZrO₂ catalyst. The low intensity of the peak could be due to the low La content in our catalysts (5%) compared to the Ni/La₂O₃ used in the previous investigations [16,17].

It was also observed in the XRD patterns of all spent catalysts (not shown here) that no peaks related to Ni containing phases were observed. However, the main peak of NiO appeared again after exposing the catalysts to air for few minutes (see Fig. 7). One could think of four different explanations: (i) formation of nickel zirconia stoichiometric phases, (ii) formation of highly dispersed Ni particles, (iii) formation of a Ni amorphous phase and (iv) formation of Ni₃C.

The formation of nickel zirconia stoichiometric phases such as Ni₃ZrO or Ni₄Zr₂O implies dissolving of NiO in the ZrO₂ lattice. It has been reported that the solubility of Ni particles in yttrium stabilized zirconia (YSZ) is much smaller when the NiO is reduced to metallic Ni [34]. The presence of a NiO peak and the absence of Ni₃ZrO ($2\theta = 37.729$ [35]) and Ni₄Zr₂O ($2\theta = 38.314$ [36]) at the diffraction pattern of the calcined catalysts at 725 °C for 15 h, suggest that stoichiometric nickel zirconia phases are not formed during reaction, at 700 °C for 20 h.

An alternative explanation could be the presence of Ni in an amorphous phase, as suggested by Nam et al. [37]. They studied methane dry reforming over Ni-based perovskite catalysts. In a similar way, no Ni or NiO peaks were observed in the XRD patterns after reaction. The absence of Ni and NiO peaks was attributed to either amorphous NiO or highly dispersed Ni particles. It was concluded that the presence of highly dispersed Ni ions in the fresh catalyst in combination with a reducing atmosphere during reaction could result in very small Ni particles even after reaction. However, highly dispersed Ni particles are not expected to be present under our reaction conditions, taking into account NiO particles sizes of the fresh catalysts (~20 nm).

The formation of Ni₃C is also proposed as a possible explanation for the absence of Ni species in the XRD patterns of the used catalysts. Bai et al. [38] observed the formation of Ni₃C crystallites at high temperatures as a result of the interaction between Ni

metal and the deposited carbon. Although, De Deken et al. [39] reported that Ni₃C is thermodynamically metastable above 400 °C they claimed a transformation from the graphitic to the carbide form during the cooling of the catalyst. The presence of Ni₃C cannot be ruled out but it cannot be observed in our experimental results due to overlapping of Ni₃C and ZrO₂ peaks. The actual reason for not observing a Ni phase as detected with XRD remains unclear.

To summarize, Ni/ZrO₂ catalysts modified with La and K are reasonably stable for the steam reforming of acetic acid by minimizing coke formation and/or deposition. They show promise for the steam reforming of more complex biomass derived oxygenates, which are currently under study.

5. Conclusions

It has been shown that Ni/ZrO₂ is an active catalyst for the steam reforming of biomass related oxygenates. However, it loses activity with time on stream, as a result of deactivation for both the steam reforming and WGS reactions. WGS seems to be more susceptible to deactivation than steam reforming. Carbon deposition is suggested to be the cause of the deactivation. Addition of potassium and/or lanthanum improves the catalyst life, resulting, in the case of La-based catalysts, in a better performance than the commercial pre-reforming catalyst. Addition of potassium is suggested to enhance gasification of carbonaceous species by facilitating the formation of reactive hydroxyl groups. La is proposed to enhance coke combustion by forming oxygen-containing species during reaction (La₂O₂CO₃).

Acknowledgements

The authors thank Dr. I. Babich and Ir.G. van Rossum for useful discussions. We thank Ing. L. Vrielink, Dr. J.M. Dekkers, Dr. M. Smithers and Dr. E.G. Keim for characterization. Financial support from ACTS (053.61.007) is gratefully acknowledged.

References

- [1] K.-A. Adamson, *Energy Policy* 32 (2004) 1231–1242.
- [2] F. Bimbela, M. Oliva, J. Ruiz, L. Garcia, J. Arauzo, *Journal of Analytical and Applied Pyrolysis* 79 (2007) 112–120.
- [3] G. van Rossum, S.R.A. Kersten, W.P.M. van Swaaij, *Industrial & Engineering Chemistry Research* 46 (2007) 3959–3967.
- [4] C. Rioche, S. Kulkarni, F.C. Meunier, J.P. Breen, R. Burch, *Applied Catalysis B: Environmental* 61 (2005) 130–139.
- [5] D. Sutton, B. Kelleher, J.R.H. Ross, *Fuel Processing Technology* 73 (2001) 155–173.
- [6] K. Takanabe, K.-i. Aika, K. Seshan, L. Lefferts, *Chemical Engineering Journal* 120 (2006) 133–137.
- [7] K. Takanabe, K. Aika, K. Seshan, L. Lefferts, *Journal of Catalysis* 227 (2004) 101–108.
- [8] K. Takanabe, K.-i. Aika, K. Inazu, T. Baba, K. Seshan, L. Lefferts, *Journal of Catalysis* 243 (2006) 263–269.
- [9] J.R. Rostrup-Nielsen, *Catalysis: Science and Technology* 5 (1984) 1–117.
- [10] M.A. Henderson, *Surface Science Reports* 46 (2002) 1–308.
- [11] J.H. Larsen, I. Chorkendorff, *Surface Science Reports* 35 (1999) 163–222.
- [12] M. Marquievich, X. Farriol, F. Medina, D. Montané, *Catalysis Letters* 85 (2003) 41–48.
- [13] P.N. Kechagiopoulos, S.S. Voutetakis, A.A. Lemonidou, I.A. Vasalos, *Energy Fuels* 20 (2006) 2155–2163.
- [14] J.W. Snoeck, G.F. Froment, M. Fowles, *Industrial and Engineering Chemistry Research* 41 (2002) 3548–3556.
- [15] N.V. Parizotto, R.F. Fernandez, C.M.P. Marques, J.M.C. Bueno, *Studies in Surface Science and Catalysis* 167 (2007) 421–426.
- [16] S.G. Chen, R.T. Yang, *Energy Fuels* 11 (1997) 421–427.
- [17] Z. Zhang, X.E. Veykios, *Applied Catalysis A: General* 138 (1996) 109–133.
- [18] J. Guo, H. Lou, Y. Zhu, X. Zheng, *Materials Letters* 57 (2003) 4450–4455.
- [19] H. Schaper, E.B.M. Doesburg, L.L. Van Reijen, *Applied Catalysis* 7 (1983) 211–220.
- [20] N.S. Figoli, P.C. Largentiere, A. Arcoya, X.L. Seoane, *Journal of Catalysis* 155 (1995) 95–105.
- [21] A.C. Basagiannis, X.E. Veykios, *Applied Catalysis A: General* 308 (2006) 182–193.
- [22] J.R. Galdamez, L. Garcia, R. Bilbao, *Energy Fuels* 19 (2005) 1133–1142.
- [23] D.L. Trimm, *Catalysis Today* 49 (1999) 3–10.

- [24] K.G. Azzam, I.V. Babich, K. Seshan, L. Lefferts, *Journal of Catalysis* 251 (2007) 153–162.
- [25] J. Comas, F. Mariño, M. Laborde, N. Amadeo, *Chemical Engineering Journal* 98 (2004) 61–68.
- [26] F. Auprêtre, C. Descorme, D. Duprez, *Catalysis Communications* 3 (2002) 263–267.
- [27] K. Norman, Sandia report, 2007, 37.
- [28] L.K. Mudge, E.G. Baker, D.H. Mitchell, M.D. Brown, *Journal of Solar Energy Engineering, Transactions of the ASME* 107 (1985) 88–92.
- [29] F. Frusteri, S. Freni, V. Chiodo, L. Spadaro, O. Di Blasi, G. Bonura, S. Cavallaro, *Applied Catalysis A: General* 270 (2004) 1–7.
- [30] F. Arena, F. Frusteri, A. Parmaliana, *Applied Catalysis A: General* 187 (1999) 127–140.
- [31] F.R. van den Berg, M.W.J. Craje, A.M. van der Kraan, J.W. Geus, *Applied Catalysis A: General* 242 (2003) 403–416.
- [32] C.-K. Kuei, J.-F. Lee, M.-D. Lee, J.W. Geus, *Chemical Engineering Communications* 101 (1991) 77–92.
- [33] U. Olsbye, O. Moen, A. Slagtern, I.M. Dahl, *Applied Catalysis A: General* 228 (2002) 289–303.
- [34] D. Linderöth, *J. Am. Ceram. Soc.* 84 (2001) 2652–2656.
- [35] R. Mackay, H.F. Franzen, *Journal of Alloys and Compounds* 186 (1992) L7–L10.
- [36] R. Mackay, G.J. Miller, H.F. Franzen, G. Haemers, *Journal of Alloys and Compounds* 204 (1994) 109–118.
- [37] H.C. Nam, S.H. Lee, H. Jung, K.Y. Lee, *Studies in Surface Science and Catalysis* 119 (1998).
- [38] Z. Bai, H. Chen, B. Li, W. Li, *International Journal of Hydrogen Energy* 32 (2007) 32–37.
- [39] J. De Deken, P.G. Menon, G.F. Froment, G. Haemers, *Journal of Catalysis* 70 (1981) 225–229.